Acute Radiation Risks Tool (ARRT) Development for the Upcoming Human Exploration Missions

S. Hu[1], S. Monadjemi[2], J. E. Barzilla[3], and E. Semones[4]

[1]KBR, Houston, TX.
[2]Washington University in St. Louis, St. Louis, MO.
[3]Leidos, Houston, TX.
[4]NASA Johnson Space Center, Houston TX.

Corresponding author: Shaowen Hu (shaowen.hu-1@nasa.gov)

Key Points:

- An algorithm to use onboard dosimeter readings to assess acute risks for future space exploration missions is developed into a web tool
- This tool represents a good example of effort to transition research to operations
- Many state-of-the-art facilities of full stack web applications and advanced computational techniques are essential to the development

Abstract

The health risks of space radiation present big challenges to space exploration, with the possibility of large Energetic Solar Particle Events (ESPEs) inducing Acute Radiation Sickness (ARS) during upcoming Artemis missions. An operational software Acute Radiation Risk Tool **(**ARRT) was developed to directly use measurements from onboard dosimeters to project organ doses during times of increased radiation exposure, so that any possible ARS risks of the astronauts can be modelled and monitored in real time using a data stream at the astronaut location. To enable ARRT to handle variant scenarios of any possible ESPEs in an automatic manner for mission operation, two datasets were employed in developing its modules, one involving historical solar protons recorded over the past four decades, and the other using the real-time telemetry readings of dosimeters onboard International Space Station (ISS). Though vastly different in term of data cadence, smoothness, and data gaps, all events in these datasets can be correctly processed to output organ doses and ARS risks and generate flight notes for communication within the Flight Control Team (FCT). All these tasks are completed with close interactions between multiple modules developed with many state-of-the-art facilities of full stack web applications. This work demonstrates that ARRT meets the requirement to project radiation exposure and to provide clinical guidelines in very short time steps as the ESPE unfolds, even for the longest event in datasets, making this tool eligible to be tested during the upcoming unmanned Artemis mission and utilized in future space exploration.

Plain Language Summary

An operational tool ARRT was developed to directly use the onboard dosimeters' reading as inputs to estimate organ dose and possible clinical acute effects in case of severe Solar Particle Events (SPEs) for the upcoming Artemis missions. This paper describes all underlying models of the tool, various functions essential to operational management of possible effects, and how they are integrated to run automatically in real time whether the dosimeter readings are at background range or are elevated. A historical dataset with recorded 159 significant events is used to demonstrate its flexibility and accuracy to process diverse features of SPEs.

1 Introduction

Leaving the protection of the Earth’s atmosphere and geomagnetic field, astronauts travelling in deep space are at risk from radiation hazards induced by various high energy particles ubiquitous in our solar system. In the literature, much of the focus has been on the high energies of Galactic Cosmic Rays (GCR), which are hard to shield and may induce stochastic late health effects such as cancers that are of post-flight concern. Additionally, the intense Energetic Solar Particle Events (ESPEs) can cause Acute Radiation Sickness (ARS) that could manifest during the mission. Previous analyses indicate that ARS symptoms would be generally mild to moderate even in the worst case SPEs for crew inside a typical interplanetary spacecraft (Townsend et al., 1991, 2018), but even mild manifestations of fatigue and nausea could make the impacted crew less able to perform required tasks and thus may adversely impact the success of a mission (Hu et al., 2009). As opposed to GCR, SPEs can be effectively shielded against, and recent vehicle designs have incorporated shielding concepts that make use of the redistribution of vehicle mass.

An effective warning system for a large SPE could also allow the crew additional time to reconfigure the vehicle volume and reduce their event exposure.

As SPEs are not always directed to the measuring satellites deployed either close to the Earth or in interplanetary space, a practical way to estimate the ARS risks for future exploration spaceflights like Mars missions will be through the use of onboard dosimeters. Using direct measurements, radiation exposure can be monitored both in real-time and always along the path of the spacecraft. Such an algorithm has been developed specifically for the Orion Multi-Purpose Crew Vehicle (MPCV) and described in a recent publication (Mertens et al., 2018). This organ dose estimation algorithm involves a fitting procedure between the real-time vehicle dosimeter measurements and a precomputed database of dose quantities calculated from the HZETRN radiation transport code (Slaba et al., 2016; Wilson et al., 2016), considering the actual MPCV vehicle geometry and mass distribution. The paper also described how the estimated organ doses at the crew locations are utilized as inputs to a set of biological response models, which predict clinically critical syndromes associated with ARS and quantify Radiation-Induced Performance Decrement (RIPD) (Hu & Cucinotta, 2011; Hu et al., 2009, 2012). The modeled results will provide important information to guide the crew mitigation efforts in case of severe ESPEs through the efforts of FCT.

The organ dose fitting algorithm, as well as the biomathematical ARS models, have been incorporated in a software package, the Acute Radiation Risks Tool (ARRT), which is currently planned to test operationally on NASA's next unmanned beyond-Low Earth Orbit (LEO) mission (Artemis I at the time of this writing) and will be fully utilized on the following manned beyond-LEO mission (Artemis II at the time of this writing) (Hu et al., 2020). During a space flight mission, ARRT will be run at the Mission Control Center (MCC), and all its outputs will be automatically produced at the telemetry time cadence of the vehicle dosimeter measurements, which is anticipated in the range of 15 to 30 minutes. The operationally useful functions of the tool include rendering and plotting the dosimeter readings, detecting the onset and end of an event, calculating and plotting the relevant organ dose quantities, triggering the ARS biological models if threshold is reached, and generating a flight note to facilitate communication of a mitigation response within FCT. This paper attempts to give a summary of these functions and to describe how they are developed in a compact software tool. Section 2 briefly describes the algorithms underlying various models, Section 3 summarizes the strategies used to develop various modules and the functions of each module, while Section 4 gives examples of the outputs of a historical dataset.

2 Modeling algorithms

This section describes the algorithm of the two main components of ARRT. The method of estimating the ESPE organ doses from the vehicle dosimeter measurements is presented in section 2.1. A brief summary of the acute biological response model is given in section 2.2, the inputs of which come from the ESPE organ dose model.

2.1 SPE organ dose estimation

ARRT is developed specifically for the MPCV, an interplanetary spacecraft intended to carry a crew of four astronauts to destinations at or beyond LEO. The on-board radiation detection of this spacecraft will be provided by the Hybrid Electronic Radiation Assessor (HERA), which is a distributed dosimeter system based on the coupling of solid-state silicon detectors with the Timepix chips (Kroupa et al., 2015). In the upcoming Artemis I uncrewed flight, one HERA system with three detectors will be deployed at different locations. For Artemis II, the first scheduled crewed mission of MPCV, two HERA systems with six spatially separated sensors will be deployed for more robust measurement (Figure 1).

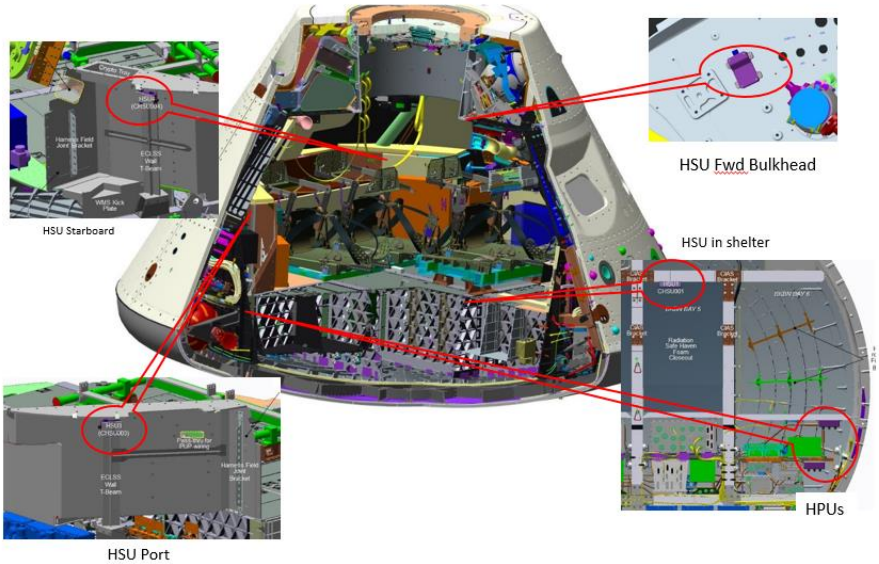

Figure 1. 6 HERA detectors at various locations of MPCV. HPU = HERA Processing Unit. HSU = HERA Sensor Unit.

ESPE effects can be mitigated during the vehicle design process through thoughtful redistribution of mass to provide a secondary role in radiation shielding. The NASA Space Radiation Analysis Group (SRAG) has been closely involved with the design process of the MPCV to identify locations with lower inherent shielding and attempt to improve the overall shielding concept without adding excess mass to the vehicle. In addition to improving the design of the vehicle, a contingency location has been designated where the crew can shelter in the stowage bays of the vehicle, redistributing the mass contained within this area to improve radiation protection (Figure 2).

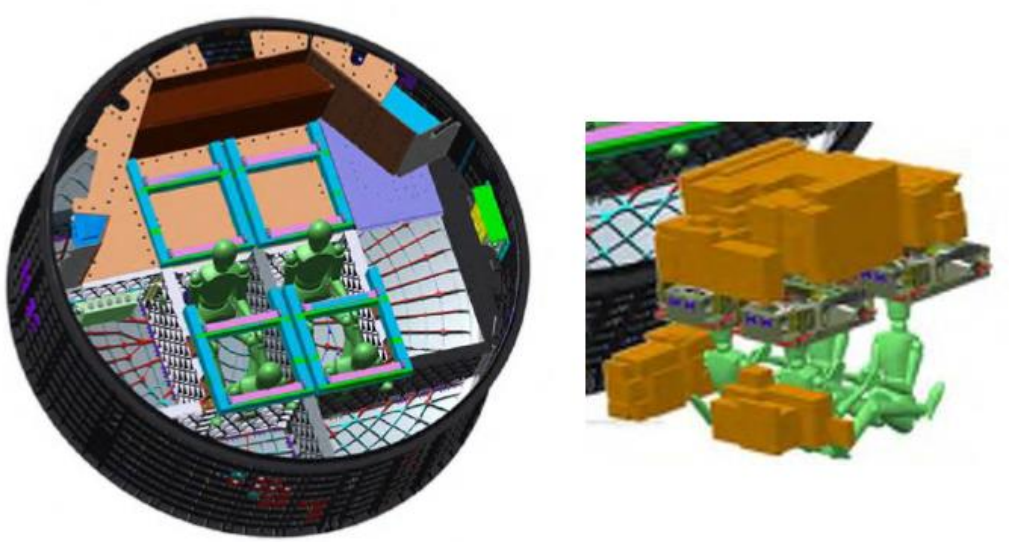

Figure 2. Schematic diagram of solar storm shelter for Orion MPCV after reconfiguration (Courtesy of Lockheed Martin Inc.).

The algorithm of organ dose estimation from dosimeter measurement has been described in detail in a previous paper (Mertens et al., 2018), which involves the following four major steps:

1. Generate a database of silicon doses at vehicle dosimeter locations and organ doses at the normal crew seat locations as well as the crew locations inside the storm shelter, for 65 historical events with known total spectra.
2. Find the event in database that minimizes the differences between measured and database averaged dose in silicon, whose spectrum thus best matches the spectral shape of the real-time vehicle radiation environment.
3. Find the optimal scaling parameters between the vehicle dosimeter measurements and the precomputed absorbed dose in silicon at the dosimeter locations for the selected event in the historical ESPE database.
4. Apply the scaling parameters to the database of organ doses to obtain real-time organ doses at the normal and storm-shelter crew locations.

The reliability of this algorithm was checked with the October 1989 event. Assuming an isotropic distribution of ESPE protons, it was found that the differences are within 2% between the total organ doses predicted by this algorithm and those calculated from the original spectrum of this event, and the uncertainty of organ dose rates is on the order of 25–35% for the 329 time intervals (30-minutes) (Mertens et al., 2018). This study also verified that the additional three vehicle dosimeters in the Artemis II configuration do not improve the accuracy of the organ dose prediction, but provide redundancy in the onboard measurements in case one or more of the dosimeters malfunction. Nevertheless, for the Artemis I configuration, if one dosimeter measurement is unavailable, the maximum difference of organ dose rates can reach 54% with two dosimeter measurement, but the uncertainty can be less than 31% if HPU1 is among them. If only one dosimeter is functioning, the error of using the dosimeter readings as organ dose rates can be as high as 20-folds (Mertens et al., 2018).

2.2 Acute biological response models

The prediction of acute biological responses to SPE exposure in ARRT is based on codes developed for ARRBOD and HemoDose (Kim et al., 2010; Hu et al., 2015). ARRBOD includes the neurovascular models (nausea and vomiting, fatigue and weakness) adapted from the RIPD models (Matheson et al., 1998), and four sets of hematopoietic models, which describe the dynamics of lymphocyte, granulocyte, leukocyte, and platelets in the peripheral blood after exposure (Hu et al., 2015). The HemoDose code is a biodosimetric tool that uses various blood cell counts after exposure to calculate absorbed doses, with a HemoGrade module linking acute and protracted doses with clinical severity scores of hematopoietic ARS, as well as the dynamics of hematopoietic stem cells in bone marrow (Hu, 2016). The user interface to these models has been modified for this work such that the Blood-Forming Organ (BFO) dose rates provided by the ESPE organ dose estimation algorithm are taken as inputs at every time point, and outputs are generated along with the real-time update of dosimeter readings.

3 ARRT development strategy

This section describes the strategies used in developing various modules of ARRT, which include reading and plotting dosimeter recordings, detecting the onset and end of an event, calculating and plotting the relevant organ dose quantities, triggering the ARS biological models, and generating a flight note for FCT.

3.1 Reading and plotting dosimeter recordings

As meaningful real-time HERA data will not be available until Artemis I and Artemis II start their journeys in space, the development of ARRT must rely on a historical dataset and a real-time dataset.

The historical dataset in ARRT is generated by transport calculation with the SEPEM 2.0 dataset (http://www.sepem.eu/), which is a cross-calibrated uniform dataset using the Geostationary Operational Environmental Satellite (GOES) measured solar proton fluxes during 1974-2015, with an energy range 5-289 MeV. With segmental spectra (Hu et al., 2016) of 15-minute cadence generated from the fluxes as a boundary condition, and material and shielding thicknesses determined by ray tracing the computer-aided design (CAD) model of the MPCV for Artemis II (with 6 HERA sensors), transport calculations through the vehicle are performed by a numerical solution of the one-dimensional Boltzmann transport equation using the HZETRN2015 code (Slaba et al., 2016; Wilson et al., 2016). The resultant dataset contains dose rates for the 6 dosimeters spanning uniformly from 1974 to 2015, with a 15-minute cadence.

At the time of this writing the web based ARRT is hosted on a Linux server inside the NASA JSC firewall, utilizing libraries such as dygraphs, PHP, JavaScript, Bootstrap, jQuery, HTML, and CSS. The simulated HERA dose rates for Artemis II configuration are stored locally with ARRT. It is assumed the Artemis I shielding configuration is the same as Artemis II, but with only 3 onboard dosimeters. The functions of reading and plotting of historical HERA data are conducted through interactive calls between codes developed in PHP, JavaScript and dygraphs. Figure 3 shows a snapshot how these interactions are performed, which is further illustrated in Section 3.5. After an event is selected in the SPE list, the onset time of the input panel is automatically set as the time 72 hours before the default onset of this event, and the HERA readings of the whole span of the event are plotted in the plot panel “HERA Reading II”, and the

7 days readings before the end of the event are plotted in “HERA Reading I”. The default values for “Factors”, “Dosimeters”, “Time Window”, “Stream Speed”, and “Refresh Frequency” are shown in Figure 3, which can be modified by the user. Dosimeters 1, 2, 3, 4, 5, 6 refer to HPU1, HPU2, HSU1, HSU2, HSU3, and HSU4, respectively. If one or more dosimeters malfunction, the user can delete the unit(s) and their readings will disappear from the plots.

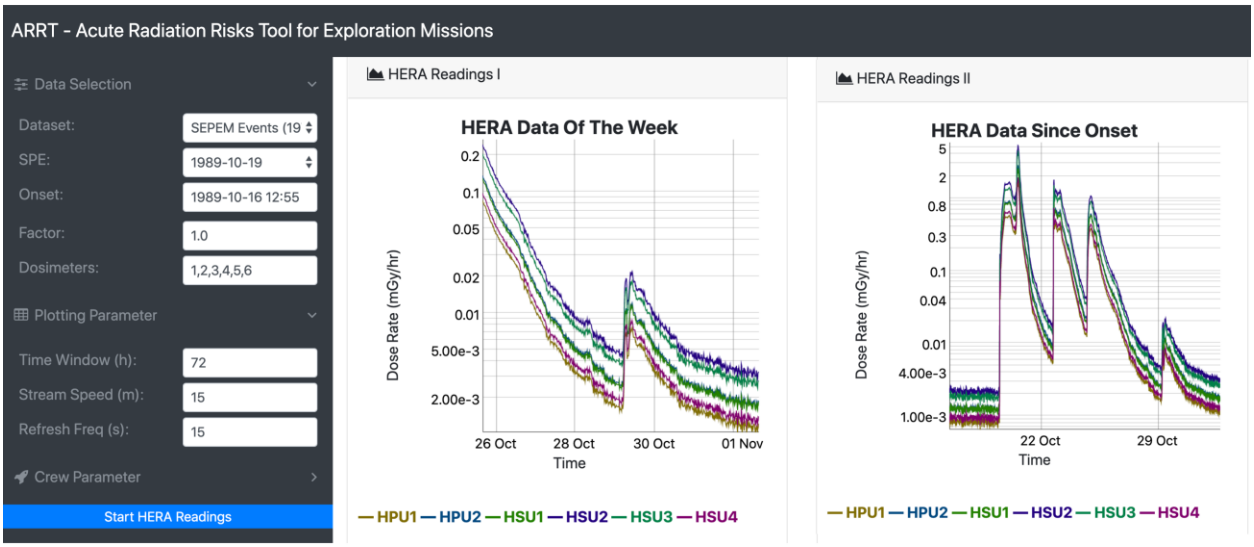

Figure 3. ARRT user input panel and HERA dose rate reading and plotting for historical SPEs

After the user clicks the “Start HERA Readings” button, both plots update at a pace set by the “Refresh Freq”. If the value of “Refresh Freq” is modified, the plotting will pause and need the user to click the “Resume HERA Readings” button to resume. If the value of “Time Window” is modified, the change will reflect in “HERA Reading II” in just one step, after that the value returns to the default 72 hours automatically. These two features were implemented to ease the usage for SRAG operations. All other modification of input values can be reflected and retained in the plots automatically. Changing the onset lets the user go to any time he/she may be interested in (within the SEPEM range 1974-2015), increasing the factor can demonstrate the effects for large SPEs, while deselecting dosimeters allows the user to view readings of fewer HERA sensors. These functions are not needed for real-time operational monitoring, as the time, factor and the dosimeters are all set in such a situation. However, ARRT can be used as an analysis tool for events just passed, such as the example illustrated in Section 3.2, showing how these functions can be utilized. Additionally, the dygraphs library used in plotting allows zooming in the plots either horizontally or vertically, which is useful to examine the details of the measurement. At the bottom of each plot, there are two links for downloading data file and displaying data in a new tab, once the plot is activated.

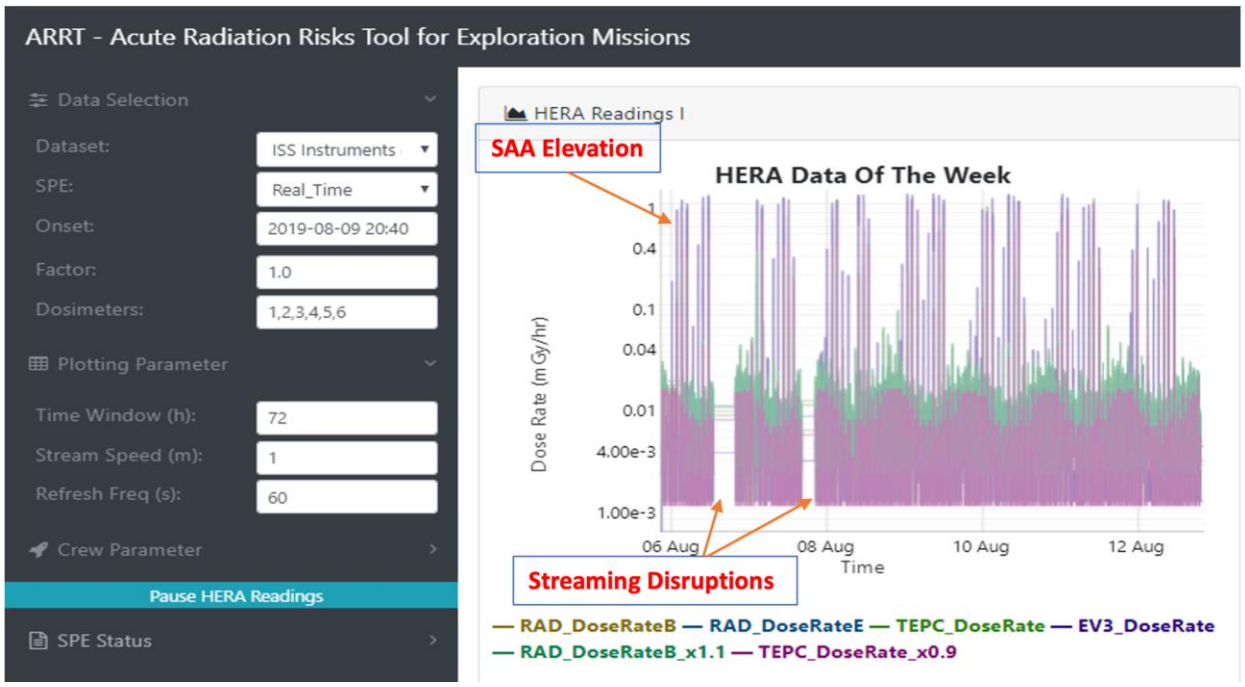

Figure 4. ARRT user input panel and HERA dose rate reading and plotting for the real-time data.

In addition to the SEPEM dataset, ARRT uses a real-time dataset by linking with the databases of International Space Station (ISS) instruments maintained by SRAG, which include dose rates measured by Radiation Assessment Detector (RAD), Tissue Equivalent Proportional Counter (TEPC), and Extra-Vehicle Charged Particle Directional Spectrometer (EV-CPDS). The dose rates in the record uniformly populate ARRT from their starting service time to the present time, with a one-minute cadence. If the user selects the "RealTime" option as shown in Figure 4 and clicks "Start HERA Readings" button right after, the ISS dataset will be streamed and plotted in real time, updated every minute. As the ISS instrument data are downlinked to a SRAG internal database, from which ARRT retrieves the data, the streaming can be disrupted for various reasons. When this happens, ARRT automatically sets the readings of the units as the last available dose rates until the connection is restored. Figure 4 shows two such incidents between August 6 and August 8, 2019. As SRAG will maintain active instrumentation data for the future Artemis I and Artemis II missions in a similar manner as for ISS, the real-time onboard dataset can be easily migrated in ARRT.

The real time data in Figure 4 are significantly different from the simulated historical data in Figure 3, because the radiation environments are different for current ISS and the GOES satellites. The ISS cruises mostly inside the Earth's magnetosphere, with an average altitude of about 410 km; therefore, the majority of radiation sources from galactic cosmic rays and solar energetic particles are effectively sheltered, especially for those with low kinetic energies. However, the strength of the magnetic field is not the same along the trajectory, therefore the measured dose rates have large oscillations. In addition, the ISS passes through the South Atlantic Anomaly (SAA) region several times every day, causing significant dose rate elevation for 5~10 minutes each time (Figure 4). For the GOES satellites, because they orbit above the

Earth at geosynchronous altitude (≈ 6.6 Earth radii, about 35,786 km), their geomagnetic effects are very minor, and SAA has no impact. The planned trajectory of Artemis I will have the vehicle orbiting the Earth and travelling through the van Allen belts before flying in free space to the moon. The vehicle will then orbit the moon and return to Earth, passing through the free space environment and the trapped radiation belts before landing. For the following Artemis II and other human exploration mission with destinations beyond LEO, the spacecraft would have a brief transit through the van Allen belts, mainly experiencing radiation environment in interplanetary space. Therefore, the HERA readings of ARRT for future missions should be more similar to the simulated historical data, without the oscillations and "spikes" as in Figure 4.

3.2 Detecting the onset and end of an event

Traditionally, the onset and end of an SPE are defined as the first and last time points of a period with continually elevated proton fluxes higher than a threshold (Feynman et al., 1990; Jiggens et al., 2012). However, because of the modulation of solar cycles, the background fluxes change significantly from the solar minimum to the solar maximum (Figure 5), and the difference of intra-vehicular dose rates can be as large as 2~3 times (Fig 3 in Norbury et al., 2019). If a fixed dose rate were chosen as the threshold to determine the onset and end of an event, the first and last time points of a same event (such as the one in Figure 5 (left panel)) would be different if it occurred at different times in solar cycles. To avoid this problem, ARRT uses the background dose rates as references for the threshold of an event, which are not fixed but varying along solar cycles.

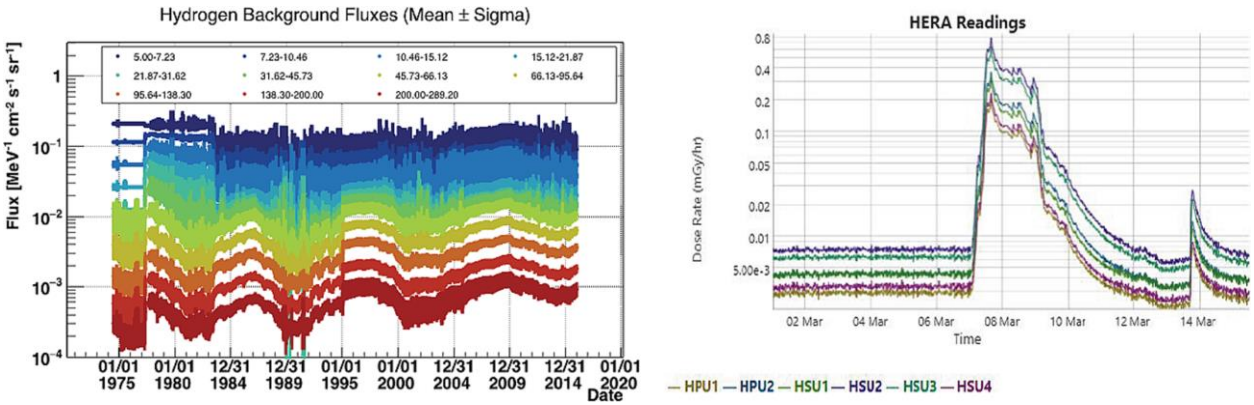

Figure 5. Variation of hydrogen background fluxes of SEPEM data (left) and HERA readings of a typical SPE (right).

To automatically calculate the background dose rates is not always straightforward, especially for the time period when multiple events occur sequentially. For the events plotted in Figure 5 (right panel), the background dose rate for the first event (with onset on Mar 07) is easy to calculate, as any time window of any length before the onset can be selected, and the mean dose rate is the correct background. However, for the second event (with onset on Mar 14), the time window cannot be selected between Mar 07 and Mar 14, as the dose rates in this time period are elevated by the first event. In ARRT, an algorithm is developed such that a one-week window is selected to calculate mean dose rate and the number of points below the mean. If the number of

points with dose rates below the mean is less than 55% of the total number of points in this time window, it is certain that there are no SPEs during this window and the calculated mean is the background dose rate. Otherwise the time window shifts one week or additional weeks behind until the condition is satisfied. This algorithm has been tested for SEPEM generated HERA readings and the calculated backgrounds are stable and independent from the occurrence of SPEs.

For the historical dataset, the threshold for SPEs is defined as the two times the background dose rate, and the onset of an event is defined as a time point with two consequential dose rates above the threshold. Currently, for the real-time SPE, the definition of onset is the same, but the threshold has to be defined as 200 times the background, because a lower threshold would misinterpret the dose-rate elevation when ISS passes SAA as an SPE (Figure 4). As ISS travels inside the Earth's magnetosphere and no significant SPE has been recorded to date, we developed code to simulate a simple event with specific starting time, hours to the peak, hours to the end, and a factor that times the original data. With these virtual events, ARRT can check if the real-time data works for the organ dose fitting module and acute risk modeling module. Figure 6 shows such an event starting at 2019-04-15 00:00, with 1 hour to the peak, 240 hours to the end, and 500 times of the original readings at the flux peak. Because the code modifies the readings with a simple linear rising from background to peak, and the threshold is defined as 200 times of the background, the detected onset of this event is 2019-04-15 00:28, as shown in Figure 6. Before the onset, the "SPE Status" is in a "Nominal" mode with a green light. When the data reading reaches the onset, ARRT enters an "Event in Progress" mode with a red light in "SPE Status" (Figure 6), the time value in the "Onset" box becomes fixed, and the "Time Window" value keeps increasing at a pace set by the "Stream Speed" and "Refresh Freq". In the meantime, the plot in "HERA Reading II" shifts its origin to the onset, displaying the readings sequentially since onset, while the plot in "HERA Reading I" continues streaming with time for one week's readings. This "Event in Progress" mode works similarly for the 159 recorded SPEs in historical dataset, but with different thresholds.

Figure 6. "Event in Progress" mode for a virtual event with the real-time dataset.

As reported by other researchers (Feynman et al., Tylka et al., Jiggens et al., 2012), many consecutive events are not independent in time, and a minimum dwelling time parameter (e.g., 24 hours in Jiggens et al. 2012) is needed so that they could be treated as the same event. Based on SRAG's operational guidance, ARRT chooses a two-hour dwelling time to determine if consecutive events can be treated as different events, and the end of an event is defined as a time point following two hours of dose rates below the threshold, for both the historical and real-time datasets. When the end is reached, ARRT goes back to "Nominal" mode with a green light in "SPE Status", the time value in the "Onset" box changes to an unfixed onset, and the "Time Window" value returns to the default 72 hours, accompanying with the changes in the plots in nominal mode. As all effects of the previous event is reset once it reaches the end, there is a health risk issue if the event is big enough to induce ARS. To remedy this problem, a dose-dependent monitoring time parameter is introduced using the following formula:

$$\text{monitoring time (hours)} = 24.0 * (\text{total dose (mGy-eq)} / 50.0)$$

For events with total BFO dose > 250 mGy-eq, which is the threshold of ARS induction for terrestrial radiation, the health effects will be monitored at least 5 days. For these rare large events, when the end is reached, ARRT goes to a "Crew Monitoring" mode with a yellow light in "SPE Status", and the time values in the "Onset" box and "Time Window" box are maintained as in "Event in Progress" mode until this monitoring period finishes. In this way, the impacts of big events to the health of crew are preserved for complete analysis. An example for this treatment will be discussed below, to demonstrate how large consecutive events can be analyzed correctly.

3.3 Calculating and plotting organ dose quantities

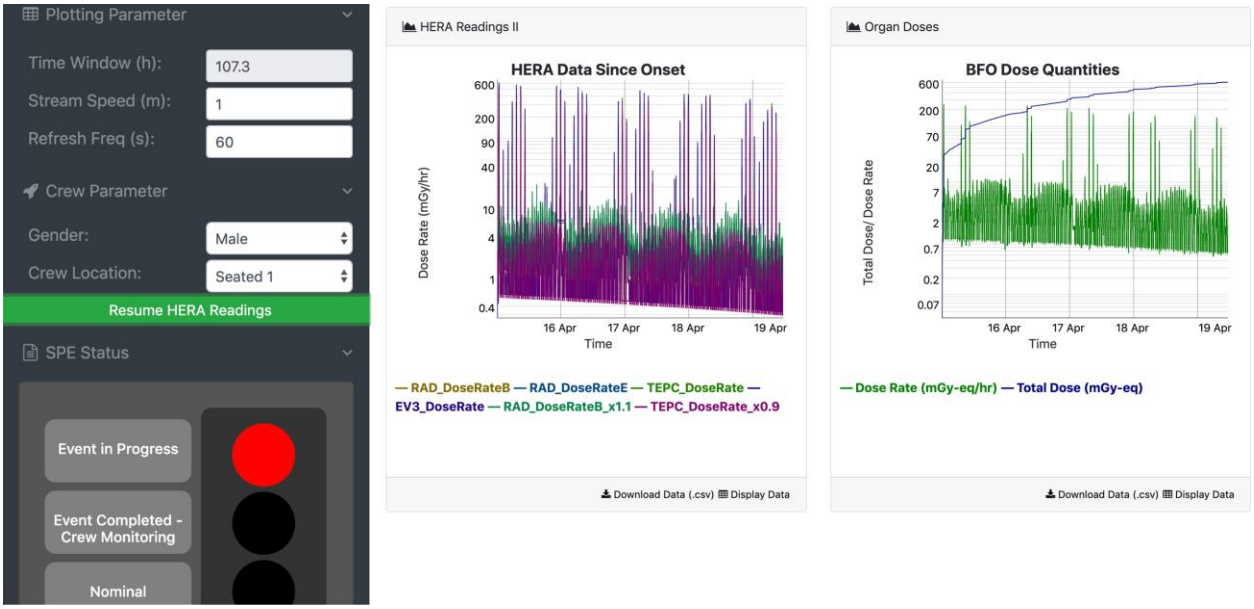

Figure 7. Plot of organ dose calculation for a male astronaut at "Seated" location 1.

Whenever an SPE is detected, a set of code is launched to project organ doses from dosimeter measurement. This is a complicated process with each step involving spectral matching in a precomputed dose database, scaling factors fitting between the vehicle dosimeter measurement and the precomputed dose quantities of the matched event, and linear scaling of the precomputed organ dose quantities (Mertens et al., 2018), which is summarized in Section 2.1. The output of each step of calculation include 27 organ doses at 8 locations in MPCV (4 nominal seats and 4 sheltered seats), for male and female astronauts respectively (Mertens et al., 2018). To reduce the amount of computation for this step, two input parameters are introduced, i.e., the "Gender" and the "Crew Location", allowing the user to check some subtle variations for different genders and locations in different runs. Figure 7 shows the output of a calculation for a male astronaut at "Seated" location 1 of the virtual event with onset on 2019-04-15 00:28, which was paused at 107.3 hours after onset. The organ dose plot includes 107.3×60 BFO dose rates and accumulative doses since the onset of the event, as the cadence is 1 minute.

As ARRT is a real-time operational tool for the exploration missions, all calculations are required to finish along with the streaming of dosimeter reading. For the real-time data such as those showing in Figure 7, all 107.3×60 steps of organ dose computation are required to finish within one minute (the cadence of data streaming). We found this could not be done with sequential code, or by breaking the code into sections with each conducting a small number of times calculation, or by parallelizing the code to use all nodes simultaneously. The solution was found by running the sequential code just in the background of the Linux system, and an unlimited number of processes are spawned to the backend cluster at a same time. The speed of calculation in this way is the fastest among all trials. However, for longer duration events, the calculation will cause a delay in the update of the plots, as additional time is needed to plot 1-week HERA data, to plot HERA data since onset, to perform ARS calculation and plotting, and to generate flight notes. If this is the case, the user can increase the "Stream Speed" and the corresponding "Refresh Freq" inputs to allow longer gaps between reading dosimeter data, i.e., by manually increasing the default cadence, so that all tasks can be finished properly within the

cadence. For historical SEPEM dataset, such problems are not presented as the cadence is 15 minutes and long enough to conduct the required computations even for the event of longest duration. At the time of this writing, the Linux server hosting the code has only 32 CPUs. Once the code is migrated into a server with more CPUs, the speed limit should be lifted.

3.4 Triggering the ARS biological models

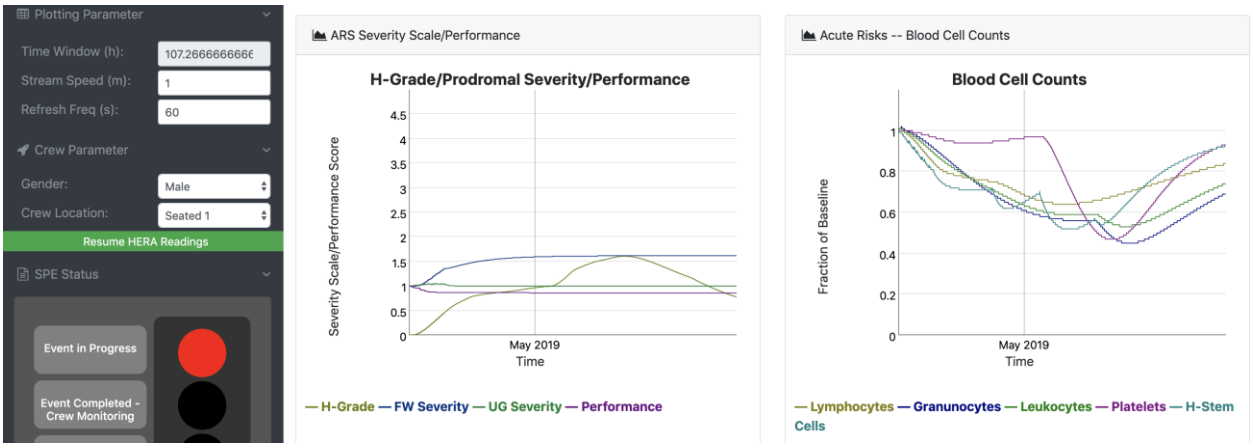

Figure 8. Plot of ARS projections for a male astronaut at "Seated" location 1, if encountering a virtual event depicted in Figures 6 and 7.

Early radiobiological studies suggested all ARS symptoms are deterministic effects that manifest only above a threshold (NAS, 1976). For example, the widely used RIPD software set 0.5 Gy as the threshold to trigger two neurovascular models (Matheson, 1998). However, later investigations indicated the damages to the radiosensitive systems have no threshold limit; at low dose levels, these changes may be localized or transient, and/or they may be repaired; at high dose radiation, they may be more widespread, severe and persistent (Fliedner, et al., 2001). Therefore, ARRT does not set a threshold for the incorporated ARS models, but generates results of various endpoints whenever an ESPE occurs.

For the virtual event described above, the total BFO dose is about 600 mGy-eq for a male astronaut at "Seated" location 1 after 107.3 hours' exposure (Figure 7). Figure 8 shows various ARS effects that ARRT projects, from the onset of the event to up to 42 days (1000 hours) after the onset. The left plot displays ARS severity and performance prediction, updated in every step of real-time data reading (i.e., 1 minute). This includes H-grade (HemoGrade), severity scale of UG (upper-gastrointestinal) and FW (fatigue and weakness) symptoms, and PD (performance decrement). HemoGrade is modeled based on the changes of peripheral blood cell counts after radiation exposure (Hu, 2016). It indicates the extent of damage to hematopoiesis and the corresponding prognosis for autologous recovery, and it can be used to suggest optimal therapeutic treatment (see Table 1). UG and FW symptoms are outputs of two neurovascular models adapted from the RIPD models (Matheson, et al., 1998), describing severity of nausea and vomiting, fatigue and weakness in numerical scales (Table 2). Performance is defined as the baseline time for a healthy crew to complete a task divided by the time taken to complete the task when ill. Calculation of PD is based both on the severity of symptoms and the mental/physical difficulty of the crew's assigned tasks. A PD greater than 0.75 is considered "Effective", 0.25 to 0.75 is "Performance Degraded" and below 0.25 is "Ineffective" (Matheson, et al., 1998). For the

virtual event at around 107.3 hours since onset, the HemoGrade steadily increases from 0 to 1 during the first week, stays at level 1 for the second week, then increases to peak at 1.5 and decreases to 1 during the third and fourth weeks, and maintains at level 1 till the 42 days (Figure 8), indicating mild to moderate injury to the hematopoietic system with certain autologous recovery (Table 1). The FW score increases to 1.5 for the first week after onset, and maintains at the level till 42 days, while UG and performance results show minimal or no impact at this level of exposure (Figure 8 and Table 2).

Table 1. Textual descriptions of the HemoGrade severity level and prognosis and therapeutic options

Grading	Extent of impairment	Prognosis	Therapeutic options
H0	No damage	No observable symptoms	No need for hematopoietic treatment
H1	Mild damage	Autologous recovery certain without critical phase*	No need for hematopoietic treatment
H2	Moderate damage	Autologous recovery certain with low risk critical phase	Blood component therapy if indicated by bleeding, or appropriate antibiotic agents to cope with bacterial infections
H3	Severe damage	Autologous recovery certain with high risk critical phase	Same as those in H2. Additionally cytokines/growth factors should be administered as early as possible
H4	Fatal damage	Autologous recovery most unlikely	Stem cell transplantation, supplemented by all other supportive hematopoietic treatment

*Critical phase is defined as the duration with constant cell counts below the normal range, resulting high or low risks of developing bleeding or infectious diseases.

Table 2. Textual descriptions of the symptom severity level of prodromal radiation sickness

Severity Level	Nausea/Vomiting	Fatigue/Weakness
1	No effect	No effect
2	Upset stomach, clammy and sweaty, mouth waters	Somewhat tired, with mild weakness
3	Nauseated, considerable sweating, swallows frequently to avoid vomiting	Tired, with moderate weakness
4	Vomited once or twice, nauseated, and may vomit again	Very tired and weak
5	Vomited several times, including the dry heaves, severely nauseated, and will soon vomit again	Exhausted, with almost no strength

The right plot in Figure 8 describes the modeled dynamics of various blood cell counts at this scenario, which are expressed as ratios to their baseline counts. These are generated by the four hematopoietic models used in the HemoDose software (Hu et al., 2015). In addition to the counts of lymphocytes, granulocytes, leukocytes, and platelets from the onset to the 42 days , the time

course of the number of hematopoietic stem cells is also reported as one endpoint of the models (Hu et al., 2012), which is an indicator of the possible autologous recovery of this system (Fliedner et al., 2002). All these outputs are updated at each step of dosimeter data reading (i.e., 1 minute), along with the calculation of ARS severity scale and performance, giving updated information of the possible health outcomes of the crew and providing instant guidelines to the ground FCT. However, it is not certain if a hematological analyzer will be onboard in future exploration missions. If such a device is available, the cell counts in peripheral blood can be used to verify the projected dose as the HemoDose tool does (Hu et al., 2015). In addition, they can serve as real time biomarkers to assess ARS and develop clinical guidelines. An additional merit of the plots in Figure 8 is the projection of the critical phase, which is defined as the duration with constant cell counts below the normal range, resulting high or low risks of developing bleeding or infectious diseases. For the virtual event, the calculation indicates such phase may appear during the third and fourth weeks after the onset, giving plenty of time for the ground FCT to make decision if any medical intervention as listed in Table 1 is needed (Hu, 2016). Because SPEs can be effectively shielded, and current vehicle designs incorporate smart shielding concepts such as the redistribution of vehicle mass in MPCV, with an effective warning system for a large SPE to reduce the event exposure, it is very unlikely that astronauts inside an interplanetary spacecraft like MPCV will experience such severe health impacts that need these medical interventions (Hu et al., 2020).

Space Weather Conditions:
An ESPE was observed at 2019-04-15 00:26:00 as defined by [Flight Rule]. The mission average background dose, as monitored by HERA, is 7.10E-3 mGy/hr. As of 2019-04-19 11:46:00, the average dose rate is 3.93E+0 mGy/hr.

Recommended Crew Actions:
Based on the projected short-term crew impacts (see below) the crew is recommended to perform the Radiation Event Cabin Reconfiguration protocol and seek shelter in the storage bays per [Flight Rule].

Short-Term Crew Impacts (48 hours):
On-board instrumentation indicates that as of 2019-04-19 11:46:00, total exposure due to this ESPE was 6.90E+2 mGy. According to model predictions, a total bone marrow exposure of 6.27E+2 mGy-eq is projected. At this level, per [Flight Rule], Acute Radiation Syndrome ***is a concern for the crew***. Symptoms such as nausea and anorexia may appear within 24 hours of exposure, manifested as an upset stomach with clammy/sweaty skin and watering mouth. Complete disappearance of these symptoms is certain within 48 hours of exposure. Fatigue and mild weakness may appear during this time period. Bloodwork will indicate a mostly asymptomatic decrease in lymphocyte concentration.

The following crew impacts are expected over the next 48 hours since the onset of the ESPE*:

Symptom	**2h**	**4h**	**6h**	**12h**	**18h**	**24h**	**30h**	**36h**	**42h**	**48h**	**Incidence (%95CI)**
Nausea/Vomiting	1.00	1.00	1.00	1.01	1.02	1.02	1.01	1.03	1.03	1.03	0.00 (4.47,0.00)
Fatigue/Weakness	1.00	1.00	1.00	1.00	1.00	1.01	1.01	1.03	1.05	1.07	11.04 (45.17,1.00)
Performance Decrement	1.00	1.00	1.00	0.98	0.97	0.96	0.96	0.93	0.92	0.91	N/A
HemoGrade	0.00	0.00	0.00	0.00	0.01	0.02	0.04	0.06	0.09	0.11	N/A

*Check the reference tables for the definitions of the symptom severity levels, incidence, performance decrement, and HemoGrade.

Continuing Crew Impacts (2 days - 6 weeks):
Fatigue and weakness may persist for several weeks. The crew are at low risk of developing infectious diseases or bleeding due to a decrease in concentrations of lymphocytes, platelets, and granulocytes below the lower end of the normal range. Autologous recovery is certain.

Figure 9. Flight note for a male astronaut, if encountering a virtual event depicted in Figures 6 and 7.

3.5 Generating a flight note for ARS management

As described above, MPCV is designed with an integrated shelter. If there is a possible risk to crew health, the crew will be asked to perform the Radiation Event Cabin Reconfiguration (RECR) protocol and seek shelter in the storage bays. Generally crew shelter can be assembled in 30 minutes, and the crew can safely remain in the shelter through the event, leaving briefly as approved to conduct mission critical or hygiene-related tasks. As one of the console operators' suite of tools, ARRT will be initiated at launch and run consistently in the background. Once an ESPE is detected, the radiation console will be notified automatically and the ARS projections will be performed. This information will be used to automatically generate a Flight Note for communication with FCT, all recommendations being worked through the Flight Surgeon.

Figure 9 displays a sample flight note for a male astronaut if encountering a virtual event depicted in Figures 6 and 7. The note contains information on space weather conditions, recommended crew actions, short-term crew impacts (48 hours), and continuing crew impacts (2 days – 6 weeks). Except for the space weather conditions, all other information is generated based on the results of ARS modeling calculation. The thresholds to recommend crew action and ARS concerns are both set as 100 mGy-eq, and that for short-term crew impacts is set as 250 mGy-eq. The texts of symptoms description and recommendation are categorized into 8 scenarios based on the calculated total BFO dose from the organ dose estimation code (Supporting Information), which can be changed as the ESPE progresses in time. The table listed in flight note gives numerical scores for NV, FW, PD, and H-grade over the first 48 hours since onset, as well as incidence of the two neurovascular effects. Like the ARS plots, all texts in flight note are updated at every time step of dosimeter reading and can be downloaded in Microsoft Word format. If no increase in dose over threshold, only space weather conditions will appear in flight note, with mission background dose rate and the average dose rate of the present time, and the note download link is inactive.

3.6 Software Structure of ARRT

ARRT was developed with many state-of-the-art facilities for full stack web development, with its overall workflow depicted in Figure 10. The user interacts with an interface to set parameters of the query (i.e. time window, stream speed, etc.). Then the application loads the appropriate dataset, processes the data to check if ESPE threshold is reached, in the meantime to visualize the data and to generate flight note. Certain levels of ESPE result in additional calculations, expanded visualizations, and detailed flight notes all of which happen seamlessly by modifying SPE status and input parameters automatically (Figure 10). Regardless of the existance of an ESPE, the modules corporately run execute continuously unless if the user clicks the “Pause HERA Readings” button (Figures 4 and 6).

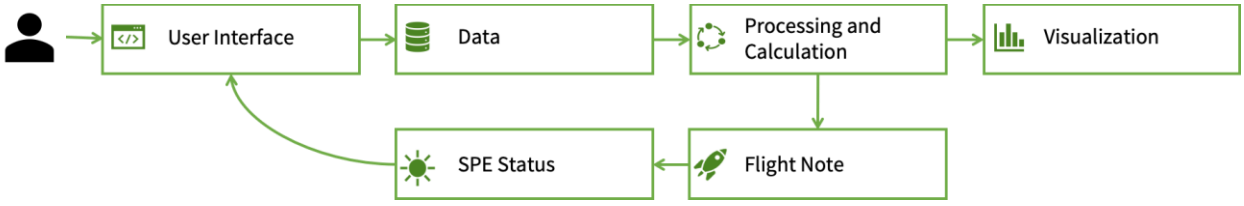

Figure 10. The overall workflow of ARRT web application.

4 ARRT operation for a typical event

The occurrence of ESPEs is hard to predict, and their developing patterns are vastly different. Table 3 lists 20 biggest events occurred between 1974 and 2015, calculated from SEPEM 2.0 dataset (http://www.sepem.eu/). It is clear that every event is unique, in term of total dose, dose rate at peak, duration, as well as the waiting time. Additionally, the time for dose rates to reach the peaks, and the time parameters for accumulative doses can be different as large as over two magnitude. To be able to process the diverse features of the events, the ARRT code should be flexible enough to deal with different scenarios, but in the meantime be robust to generate the correct results in an automatic manner. Additional challenges exist for multiple events occurring

in a short time period. To make the outcome of ARS prediction more relevant for the console operational team, it is not always easy to decide whether to treat sequential events separately or inter-dependently. The robustness of ARRT has been tested with all the simulated HERA readings from SEPEM 2.0 dataset, and for all of the 159 significant events, ARRT can correctly read and plot the data, project organ doses and ARS risks, and generate flight notes consistent with the numerical results. In the following an event with multiple sub-events is used to demonstrate how ARRT is smart to treat sequential events correctly.

Table 3. 20 biggest ESPEs during 1974-2015*

SPEs	Start Time	Dose (cGy)	DR_{Peak} (cGy/h)	Duration (h)	T_{peak} (h)	T_{10} (h)	T_{50} (h)	T_{90} (h)	$T_{waiting}$ (d)
1	1989-10-19 12:55	2.18e+01	1.15e+00	316.0	26.5	10.2	30.2	134.5	10.1
2	2000-07-13 09:25	1.32e+01	3.75e-01	153.0	48.2	27.2	32.8	49.2	31.9
3	2000-11-08 23:40	1.06e+01	9.54e-01	105.5	4.2	2.8	7.8	17.0	23.0
4	2003-10-26 17:55	9.74e+00	4.71e-01	281.2	54.5	46.8	56.8	89.8	148.1
5	1989-09-29 11:25	9.17e+00	5.73e-01	239.8	8.5	4.2	12.2	29.5	36.1
6	2001-11-04 16:25	6.49e+00	6.65e-01	111.2	34.0	5.5	29.8	36.8	11.5
7	2005-01-16 01:25	6.37e+00	2.11e+00	174.0	101.8	51.0	103.2	112.5	63.5
8	2012-03-07 02:10	4.08e+00	1.87e-01	195.5	13.2	11.2	25.2	47.8	35.8
9	1991-05-31 09:25	3.24e+00	1.11e-01	445.0	269.2	172.0	271.5	371.5	17.1
10	2001-04-15 13:55	2.73e+00	5.11e-01	118.0	1.2	1.2	4.0	65.8	2.1
11	2006-12-06 12:40	2.65e+00	5.26e-02	222.5	23.5	23.8	160.0	168.5	446.1
12	1989-08-12 15:55	2.36e+00	1.05e-01	282.2	85.2	11.5	86.0	119.0	17.1
13	1992-10-30 19:10	2.12e+00	2.45e-01	142.8	58.8	11.2	62.0	74.0	123.3
14	2001-09-24 11:40	1.94e+00	8.61e-02	141.5	20.2	11.8	23.0	39.0	36.0
15	1997-11-04 06:40	1.72e+00	3.39e-02	127.5	71.0	56.0	61.2	73.8	745.2
16	1981-10-08 00:40	1.42e+00	4.36e-02	235.2	114.2	104.0	120.5	144.0	78.3

17	1990-05-21 22:40	1.30e+00	3.86e-02	231.8	6.5	6.5	87.8	168.5	22.6
18	2002-04-21 01:40	1.20e+00	6.25e-02	115.5	8.8	3.8	12.2	31.8	106.2
19	1991-03-23 07:25	1.08e+00	2.38e-01	164.2	20.5	12.5	19.0	22.0	49.1
20	2005-09-07 21:55	1.00e+00	2.14e-02	205.0	46.2	19.0	44.2	69.2	13.5

*Based on calculation with HZETRN2015 for silicon dose rates inside a 10 g/cm^2 sphere in interplanetary space, by using spectra of every 15 minutes data from SEPEM 2.0 dataset (http://www.sepem.eu/). The onset and end times are defined similar to this paper, except for the dwelling time (24 hours). T_{peak}, T_{10}, T_{50}, and T_{90} are time parameters (hours) for dose rates reaches the peak, and accumulative dose reaches 10%, 50%, 90% of the total dose of the event, while $T_{waiting}$ is the time (days) between the end of the previous one to the onset of the present one.

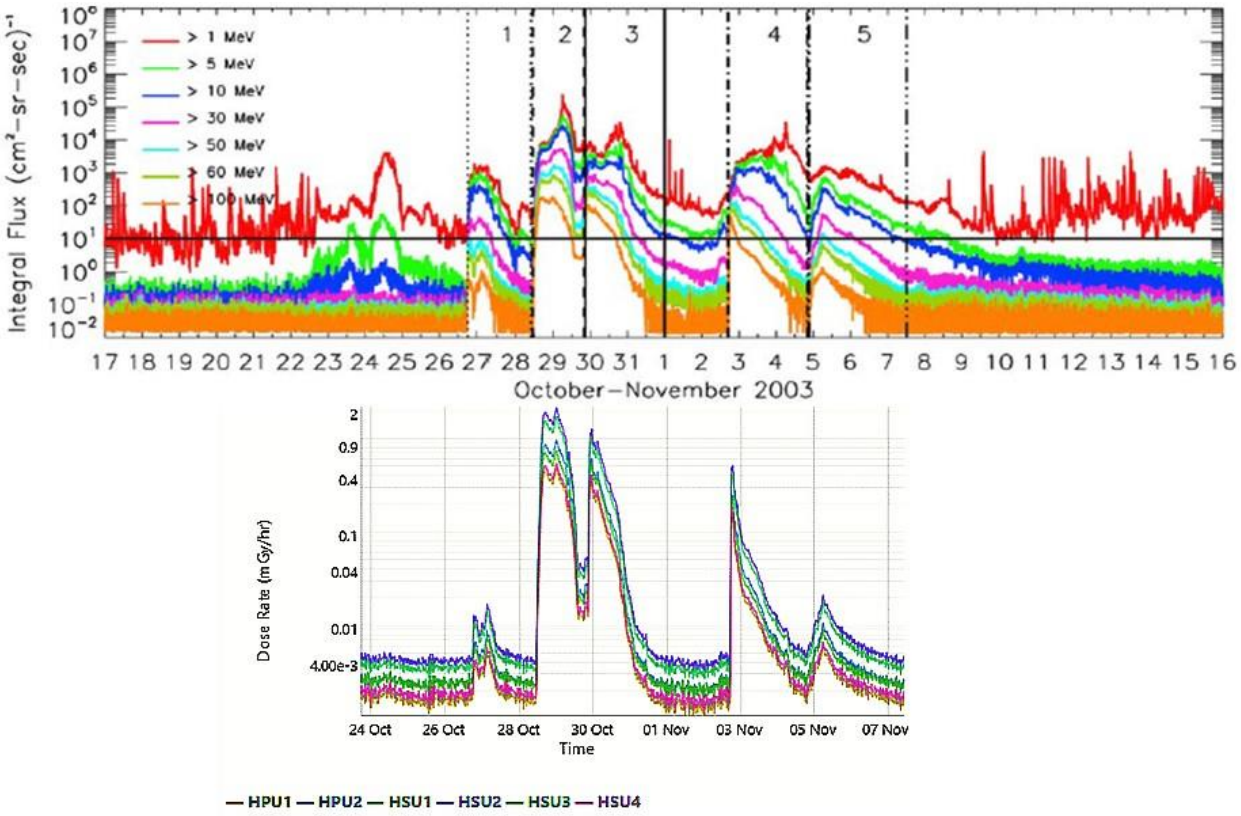

Figure 11. GOES-11 proton flux measurement of 2003-10-26 ESPE (top, adapted from Mertens et al., 2010) and ARRT simulated HERA readings (bottom).

The 2003 Halloween storm is a typical ESPE with multiple events lasting for more than 10 days, which ranks No. 4 among the biggest events during 1974-2015 (Table 3). The proton fluxes recorded by GOES detectors indicate 5 sub-events nearly overlapping with each other (Figure 11) [Mertens et al., 2010], whose onset and end times are listed in Table 4 according to different definitions. The NOAA parameters are estimated by using the proton data archived at NOAA's National Center for Environmental Information (http://www.ngdc.noaa.gov/stp/satellite/goes/index.html), which defines the start of an SPE as

when the >10 MeV integral proton flux exceeds 10 proton flux units (pfu ≡ $cm^{-2}sr^{-1}s^{-1}$) in three consecutive 5 min periods, and the end as the last time the flux was greater than or equal to 10 pfu [NOAA, 2009]. As the fluxes of >10 MeV protons between events 2 and 3 are not below the threshold (Figure 11), they should be considered as one event by this definition. As discussed above, ARRT's definition is based on the elevation of HERA dose rates within the MPCV. Because the contribution to silicon dose behind the spacecraft shielding comes mainly from protons in energy range 100-300 MeV, the onset and end times estimated by ARRT are substantially different from NOAA's. The dwelling time between event 2-3 and event 4 is about 24 hours with NOAA's definition, but increases to 58.5 hours with ARRT's definition (Table 4).

Table 4. Onset and end times for the sub-events of 2003 Halloween storm.

Sub-events	NOAA onset	NOAA end	ARRT(1)* onset	ARRT(1)* end	ARRT(20)** onset	ARRT(20)** end
1	10-26 18:35	10-27 19:40	10-26 18:10	10-27 10:25	10-26 18:10	10-27 10:25
2-3	10-28 12:25	11-01 10:50	10-28 11:40	10-31 07:10	10-28 11:40	-
4	11-02 11:05	11-04 19:40	11-02 17:40	11-04 10:25	-	-
5	11-04 22:35	11-07 12:25	11-05 00:10	11-05 17:55	-	11-12 18:55

*The factor of ARRT run is 1. **The factor for ARRT run is 20.

If the factor of ARRT run is 1, i.e., no enhancement applied to the original data, treating these events separately causes no issues for health risk analysis, as the BFO doses for these four events are 0.08, 15.5, 1.25, and 0.11 mGy-eq, respectively, all far below the threshold to trigger ARS response (i.e., 250 mGy-eq). However, if a factor of 20 is applied (for post-event analysis), the events 2-3 will generate a BFO dose of 310 mGy-eq for astronauts inside MPCV, which will induce ARS that may last 4-6 weeks (Figure 8). As events 4 and 5 will add significant doses and deteriorate the ARS in this scenario, they should be included in risk estimation together with events 2-3. There are different ways to include sub-events in an episode (Robinson et al., 2018). One simple way is to extend the dwelling time if an event reaches the threshold, and the length of the dwelling time depends on the size (i.e., dose) of the event, which is how ARRT adapts. This dose-dependent dwelling time is better than one with a fixed length, as the dwelling time (waiting time) varies significantly for different events (Table 3). Applying the threshold is important in the algorithm, as otherwise any event will lead the tool into a "Crew Monitoring" mode for a certain time, which is unnecessary if the threshold is not reached. The quantitative relationship of the dose dependence is also essential, which needs to extend the dwelling time to the time window relevant to ARS risks for significant exposure. Furthermore, the exposure induced by the following events needs to be taken account in real time, so that the duration can be further extended when total dose of the episode increases. All these considerations have been implemented seamlessly in the code of the flight note module which detects and determines the onset and end of an event.

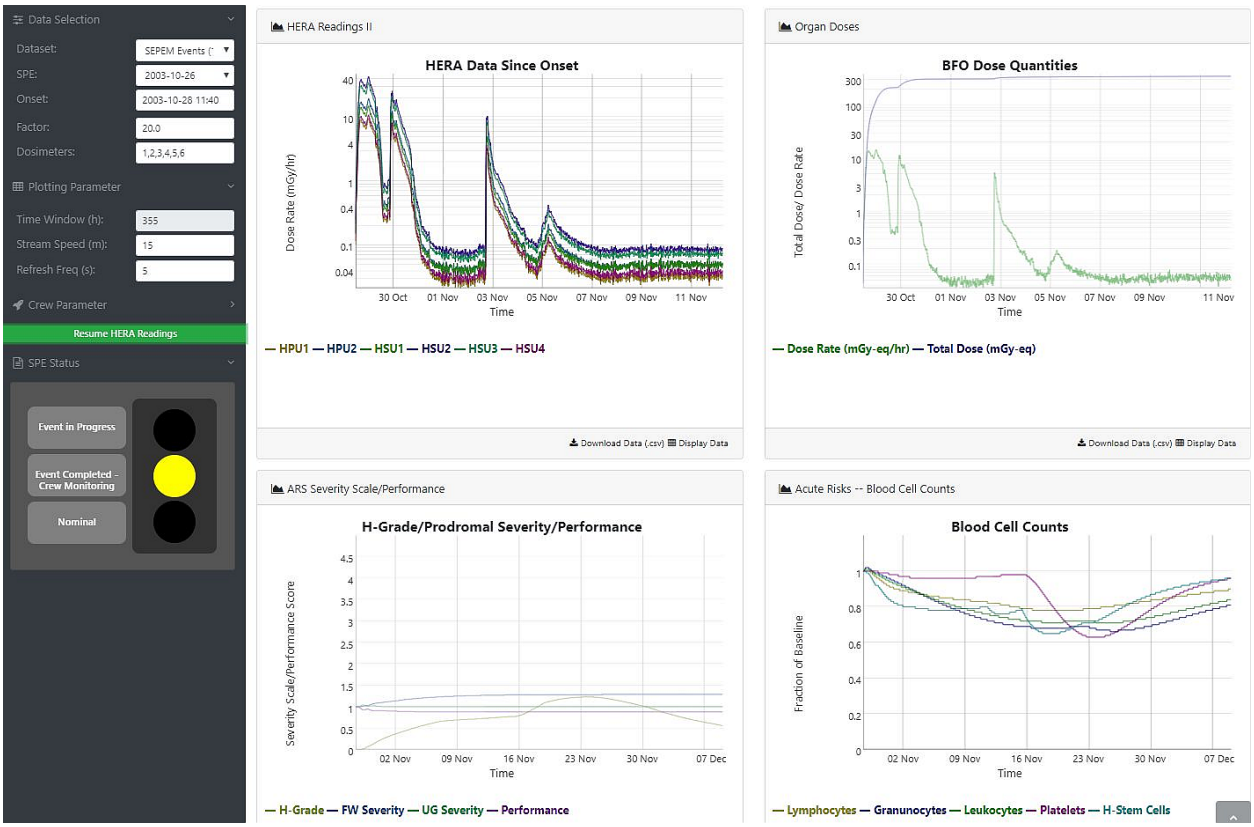

Figure 12. An ARRT run with a factor of 20 for 2003 Halloween storm. The HERA reading was paused near the end of the combined events 2-5.

Figure 12 shows a snapshot of ARRT run for an event of a magnitude of 20 times the 2003 Halloween storm. In this scenario the total BFO dose for event 1 is 1.6 mGy-eq, and it is treated as an independent event. The onset of event 2 is the same as the original data, as the background dose rates are elevated with a same factor. As the BFO dose gradually increases to over 100 mGy-eq and then over 250 mGy-eq, the flight note content for "Recommended Crew Actions", "Short-term Crew Impacts", and "Continuing Crew Impacts" change texts according to the response categories described in Supporting Information, and other contents as well as the table for the first 48 hours crew impacts are updated at each time step. After events 2-3 initially stops at 2003-10-31 7:10, the "SPE Status" changes to "Event completed, Crew Monitoring" (yellow light on). Because the total BFO dose at this stage is 310 mGy-eq, the initial dwelling time is 6.2 days (i.e., 310/50, according to the definition), so the system continues to read on data, do all kinds of calculation, and update the flight note and ARS response at every time step. If there were no following events, this monitoring mode would continue till 2003-11-06 12:00, i.e., the end of the event according to the definition of ARRT.

Because event 4 occurred on 2003-11-04 10:25, which is before the end initially determined by the total dose of events 2-3, the dwelling time set by events 2-3 is redefined according to the algorithm. When events 4 and 5 kick in, they not only add the total BFO dose, but also nullify the counter for time points below the dose rate threshold. Because the dwelling time is counted by the time points below the threshold, it is refreshed during the periods of events 4 and 5. As the total BFO dose at the end of event 5 is around 337 mGy-eq, the updated dwelling time becomes

6.74 days at this stage. That is why the end of the events 2-5 (one episode) goes to 2003-11-12 18:55 (Table 4), far later than the initially determined end time. Such a long time of crew monitoring phase is quite reasonable as the critical phase of ARS is usually 3-4 weeks after significant exposure (Hu, 2016). From the plots of ARS severity and blood cell dynamics in Figure 11, the monitoring phase covers 1/3 of the ARS projection, giving sufficient time for ground mission control team to estimate possible health effects during the following critical phase.

5 Summary and conclusion

The health risks of space radiation present the most serious challenges to space exploration, and the unpredictable ESPEs add significant radiation dose to astronauts in a short period of time, while rare large events can induce ARS requiring close crew monitoring and management even during the missions. ARRT was developed to directly use the readings of onboard dosimeters to project organ doses for the upcoming space explorations, so that any possible ARS risks to the astronauts can be modelled and monitored in real time, removing dependence on the measurements by other instruments that may not be able to detect ESPEs along the trajectories of the spacecrafts. This operational tool represents a good example of effort to transition research to operation, as many years of works in space radiation measurement and modeling, transport calculation for high energy particles, and acute radiation responses for human are involved and elegantly implemented in this compact software to be tested and utilized operationally in the upcoming Artemis missions.

To enable ARRT to handle variant scenarios of any possible ESPEs in an automatic manner for mission operation, two datasets were employed in developing its modules, one involving historical solar protons recorded over the past four decades and the other using the real-time telemetric readings of dosimeters onboard ISS. Though vastly different in term of data cadence, smoothness, and bad data gaps, all events in these datasets can be correctly processed to read and plot, to project organ doses and ARS risks, and to generate flight notes relevant to the console operational team. All these tasks are completed with close interactions between multiple modules developed with many state-of-the-art facilities of full stack web applications. As an ESPE may last days or even weeks, and all data processing, dose projection, graphic presentation, and text updates need to be performed in real-time, the computation resource for this tool is very demanding. Thanks to the fast developing computational techniques such as concurrent data structures, parallel algorithms, and multi-thread management, as well as product scalability of cloud computing platforms, which are employed in the developing process, this tool meets the requirement to project radiation exposure and to provide clinical guidelines in very short time steps even for the longest event in datasets. All these efforts make this tool eligible to be tested the upcoming Artemis missions and utilized in future space exploration.

Sources of Data and Supplementary Material

Solar proton data:

SEPEM: http://sepem.eu/help/data_ref.html

Software:

dygraphs: http://dygraphs.com/

Acknowledgements

We thank Christopher Mertens and Tony Slaba for the development of the organ dose projection algorithm for Orion MPCV. The material and shielding thicknesses files of MPCV were determined by ray tracing the CAD model by Hatem Nounu. Figure 1 was obtained from internal report by Kerry Lee, and the left panel of Figure 5 was generated by Kathryn Whitman from SEPEM dataset. This work was supported by KBR Human Health and Performance Contract (HHPC) NNJ15HK11B.

References:

Feynman, J., T. P. Armstrong, L. Dao-Gibner, and S. M. Silverman (1990), A new interplanetary proton fluence model, J. Spacecraft and Rockets, 27, 403.

Fliedner, T. M., I. Friesecke, and K. Beyrer (2001), Medical Management of Radiation Accidents—Manual on the Acute Radiation Syndrome. London: British Institute of Radiology.

Hu, S., C. Zeitlin, W. Atwell, D. Fry, J.E. Barzilla, and E. Semones (2016), Segmental interpolating spectra for solar particle events and in situ validation. Space Weather, 14 (2016), pp. 742-753, doi:10.1002/2016SW001476.

Fliedner, T.M., D. Graessle, C. Paulsen, K. Reimers (2002), Structure and function of bone marrow hemopoiesis: mechanisms of response to ionizing radiation exposure. Cancer Biother. Radiopharm., 17, pp. 405-426

Hu, S., and F. A. Cucinotta (2011), Characterization of the radiation-damaged precursor cells in bone marrow based modeling of the peripheral blood granulocytes response. Health Physics,101(1), 67–78.

Hu, S., and F. A. Cucinotta (2013), Modeling the depressed hematopoietic cells for immune system under chronic radiation. In L. E. Peterson, F. Masulli and G. Russo (Eds.), International Meeting on Computational Intelligence Methods for Bioinformatics and Biostatistics (pp. 26–36). Berlin, Heidelberg: Springer.

Hu, S., J. E. Barzilla, and E. Semones (2020), Acute radiation risk assessment and mitigation strategies in near future exploration space flights, Life Sciences in Space Research, 24, 25-33

Hu, S., M.-H. Y. Kim, G. E. McClellan, and F. A. Cucinotta (2009), Modeling the acute health effects of astronauts from exposure to large solar particle events. Health Physics,96(4), 1–12.

Hu, S., O. A. Smirnova, and F. A. Cucinotta (2012), A biomathematical model of lymphopoiesis following severe radiation accidents—Potential use for dose assessment. Health Physics,102(4), 425–436.

Hu, S., W. F. Blakely, and F. A Cucinotta (2015), HEMODOSE: A biodosimetry tool based on multi-type blood cell counts. Health Physics,109(1),54–68.

Hu, S. (2016), Linking doses with clinical scores of hematopoietic acute radiation syndrome. Health Physics,111(4), 337–347.

Jiggens, P. T. A., S. B. Gabriel, D. Heynderickx, N. B. Crosby, A. Glover, and A. Hilgers (2012), ESA SEPEM project: Peak flux and fluence model, IEEE Trans. Nucl. Sci.,59,4

Kim, M.H., S. Hu, H. N. Nounu, and F. A. Cucinotta (2010), Development of Graphical User Interface for ARRBOD (Acute Radiation Risk and BRYNTRN Organ Dose Projection). Hanover, MD: Center for Aerospace Information; NASA TP -2010-216116.

Kroupa, M., A., Bahadori, T., Campbell-Ricketts, A. Empl, S. M., Hoang, J., Idarraga-Munoz, et al. (2015). A semiconductor radiation imaging detector for space radiation dosimetry. Life Sciences in Space Research,6, 69–78.

Matheson, L. N., M. A. Dore, G. H. Anno, and G. E. McClellan (1998). Radiation-induced performance decrement (RIPD): User's manual, version 2.0 (DNA-TR-95-91). Alexandria, VA: Defense Nuclear Agency.

Mertens, C. J., B. T. Kress, M. Wiltberger, S. R. Blattnig, T. S. Slaba, S. C. Solomon, and M. Engel (2010), Geomagnetic influence on aircraft radiation exposure during a solar energetic particle event in October 2003, Space Weather, 8, S03006, doi:10.1029/2009SW000487.

Mertens, C. J., T. C. Slaba, and S. Hu (2018), Active dosimeter-based estimate of astronaut acute radiation risk for real-time solar energetic particle events. Space Weather 16, 1291–1316. https://doi.org/10.1029/2018SW001971

NASA (2014), Space Flight Hum. Syst. Stand. 1. Revision A: Crew Health. NASA Technical Standard NASASTD-3001, National Aeronautics and Space Administration, Washington, DC

NAS/NRC (1970), Radiation Protection Guides and Constraints for Space-Mission and Vehicle-Design Studies Involving Nuclear Systems. National Academy Press, Washington, DC

NOAA (2020), Solar Proton Events Affecting the Earth Environment, https://umbra.nascom.nasa.gov/SEP/, Space Weather Predict. Cent., Boulder, Colo., accessed on 2020-03-17

NRC (1967), Radiobiological factors in Manned Space flight, Report of Space Radiation Study Panel of the Life Sciences Committee, Langham WH (ed), National Academy Press, Washington, DC

Raukunen, O., R. Vainio, A. J. Tylka, W. F. Dietrich, P. Jiggens, D. Heynderickx, et al. (2018), Two solar proton fluence models based onground level enhancement observations.Journal of Space Weather and Space Climate, 8, A04.

Robinson, Z. D., J. H. Adams, M. A. Xapsos, and C. A. Stauffer (2018), Database of episode-integrated solar energetic proton fluences. J. Space Weather Space Clim., 8 A24. DOI: https://doi.org/10.1051/swsc/2018013

Slaba, T. C., J. W. Wilson, F. F. Badavi, B. D. Reddell, and A. A. Bahadori (2016), Solar proton exposure of an ICRU sphere within a complex structure: Ray-trace geometry. Life Sciences in Space Research 9, 77–83.

Townsend, L. W., J. H. Adams, S. R. Blattnig, D. J. Fry, I. Jun, M. S. Clowdsley, et al. (2018), Solar particle event storm shelter requirements for missions beyond low Earth orbit. Life Sciences in Space Research,17, 32–39.

Townsend, L.W., J. L. Shinn, and J. W. Wilson (1991), Interplanetary crew exposure estimates for the August 1972 and October 1989 solar particle events. Radiat. Res. 126, 108-110.

Tylka, A. J., J. H. Adams, P. R. Boberg, B. Brownstein, W. F. Dietrich, E. O. Flueckiger, E. L. Petersen, M. A. Shea, D. F. Smart, and E. C. Smith (1997), CREME96: A revision of the cosmic ray effects on micro-electronics code, IEEE Trans. Nucl. Sci.,44, 2150–2160.

Wilson, J. W., T. C. Slaba, F.F. Badavi, B.D. Reddell, and A.A. Bahadori (2016), Solar proton exposure of an ICRU sphere within a complex structure: Combinatorial geometry. Life Sciences in Space Research 9, 69–76.